

STUDIES ON MIXING. XXXVII.*

LIQUID FLOW AT THE BOTTOM OF A VESSEL
WITH AN AXIAL MIXER AND RADIAL BAFFLES**

I. FOŘT, V. KOZA and Z. GRAČKOVÁ

*Chemical Engineering Department,
Institute of Chemical Technology, 166 28 Prague 6*

Received January 31st, 1972

Convective liquid flow is studied below a rotating six-blade mixer with inclined plane blades, situated in the axis of a cylindrical baffled vessel. Flow regime of the charge is turbulent. The flow pattern is expressed by a field of streamlines obtained by numerical solution of the Laplace's equation for boundary condition of the first type (Dirichlet's problem). Boundaries of the region, for which the mentioned partial differential equation is solved together with the boundary conditions, are determined on a basis of the model resulting from radial distribution of axial pressures on the flat vessel bottom. The mean relative deviation of the flow pattern based on the theory and the experimental one is 21%. The field of streamlines in a system with an axial mixer and radial baffles in turbulent flow of the charge is affected primarily by the relative mixer and vessel sizes and further by the relative distance of the mixer between the vessel bottom and liquid surface. The effect of kinematic viscosity of the charge affects considerably both the flow pattern and intensity of convective flow in the studied region. The obtained results are valid for the range of Reynolds numbers $Re \in \langle 9 \cdot 0 \cdot 10^3; 2 \cdot 0 \cdot 10^5 \rangle$.

Presented description of the velocity field represents an attempt for obtaining sufficient information concerning the distribution of streamlines or the flow pattern above the vessel bottom on the basis of a relatively simple experimental measurement. It considers an axial mixer situated in a cylindrical vessel with radial baffles in turbulent flow of the charge.

The flow pattern in a mechanically mixed charge was studied for the first time by Rushton and Oldshue¹. On basis of their qualitative studies they divided the high-speed mixers rotating in a cylindrical vessel with radial baffles according to the prevailing direction of flow leaving the blades of the rotating mixer. Porcelli and Marr² have made a detailed analysis of the axial flow pattern of a propeller mixer. They have determined that in the considered system there exist two characteristic types of circulating loops forming a flow pattern: circulation intersecting the region of a rotating mixer characterizing the so-called primary flow and circulation which is not intersecting the above mentioned region and corresponding to the so-called secondary flow. These results were for the considered type of mixer experimentally confirmed³ by the study of the mo-

* Part XXXVI: This Journal 38, 1737 (1973).

** Presented at the IVth International CHISA Congress, Prague 1972.

tion of a tracer particle and by a photographic tracer method in vicinity of a rotating mixer. Similar conclusions were obtained from results of studies of a velocity field in a system with a six-blade mixer with inclined plane blades where the oriented Pitot tube or a photographic tracer method were used⁴⁻⁸. From these results was also obtained the field of streamlines in this system by a qualitative numerical solution of the Laplace equation and the assumptions resulting in description of flow by use of the above mentioned distribution of circulating loops in the system^{9,10} were confirmed. On basis of these results and experimentally determined power inputs of mixers¹¹ conclusions can be made on the most suitable arrangement of the mixed system for homogenisation process and the relation between the homogenisation effects of a mixer and its pumping effect may be determined. But these conclusions are valid only for the charge as a whole and it is not possible to make conclusions on their basis on the spacial homogeneity of the system as concerns the circulation intensity, rate of energy dissipation *etc.* as it would be possible when sufficient informations are available concerning the local conditions in an arbitrary point of the system. The measurements which, on the basis of a simple but sufficiently accurate method, give information on local characteristics at some points of the charge mixed by an axial mixer have already been made -- a method was developed and applied for measurements of local distribution of axial pressures on a flat bottom of a vessel¹². With liquid flowing in vicinity of such bottom due to the reversal of its direction the charge is acting with a force on the bottom¹³. This forced action may be used for determination of the liquid flow rate in vicinity of the bottom¹⁴. The flow rate calculated on basis of the impuls theorem for the free jet impacting on the flat plane differs from the pumping capacity of the mixer and its value depends on the geometrical conditions in the mixed system¹². It can be greater than the pumping capacity *i.e.* it may also include part of the induced flow or on the contrary it may be smaller. A more detailed description of the flow in vicinity of the bottom based on the analysis of axial pressures acting on individual parts of the bottom leads to conclusions on the liquid flow rate of the charge both below the region of the rotating mixer and at the vessel wall¹⁵.

By use of four simplifying assumptions and by combining the Bernoulli equation with the impuls theorem for a free axially symmetrical liquid jet¹⁶ a complete information on the flow rate of the charge at the bottom was obtained. This flow rate was in agreement with the flow rate in the considered region calculated from the results of direct measurements of the velocity field (determined by the Pitot tube). The detailed flow pattern formed by the streamlines from which the flow intensity in any part of the studied region could be determined have not been obtained. For such description of the spacial flow distribution the given solution does not suffice and further analysis is needed.

In this study an effort is made to find a relation between the radial distribution of axial pressures on the vessel bottom and the velocity field in the region between the rotating axial mixer and the bottom.

THEORETICAL

Let us consider a mixed system formed by a cylindrical vessel with a flat bottom with four radial baffles at the wall and with an axially situated axial mixer. The system is filled by a Newtonian charge so that the liquid surface, when at rest H , equals the inside diameter of the vessel D . The flow regime of the charge is turbulent. The coordinate system is formed by cylindrical coordinates r , φ and z with the origin situated into the intersection of the cylindrical axis of symmetry with the plane

of the bottom. The coordinate z is thus identical with the axis of symmetry and is oriented upwards. In the system defined in this way the region V_1 below the mixer is chosen (Fig. 1). The boundaries of this region are: the surface of the cylinder of radius R_0 , annular area S_1 with the radii R_0 and R_1 , area $S_2 = S_2(R, Z)$ situated between the circles with coordinates (R_1, Z_1) and (R_3, Z_3) , annular area S_3 with radii of the boundary circles R_3 and R_4 and the corresponding part of the bottom, wall and the adjacent radial baffles. The axial mixer is situated at the distance h_2 above the bottom and is rotating in such direction so as to force the charge to flow toward the vessel bottom. In the region V_1 to which our study is limited, liquid flows in such direction that it enters the region through the annular area S_1 and it leaves it through the annular area S_3 .

For the mixed system the following simplifying assumptions are made: 1) The mixed charge is incompressible; 2) system is axially symmetrical; 3) liquid flow is steady; 4) system is exchanging mass with the surrounding only through areas S_1 and S_3 ; 5) flow in the system is considered to be irrotational.

Let us now define dimensionless numbers by relations*:

$$R \equiv r/D, \quad Z \equiv z/H, \quad (1a,b)$$

$$W_{ax} \equiv \bar{w}_{ax}/\pi dn, \quad W_{rad} \equiv \bar{w}_{rad}/\pi dn, \quad (2a,b)$$

$$\Psi \equiv \psi/nd^3. \quad (3)$$

The continuity equation for the considered system may be written in the form¹⁶

$$\partial(RW_{rad})/\partial R + \partial(RW_{ax})/\partial Z = 0 \quad (4)$$

and the field of streamlines in the region V_1 may be expressed by the Laplace equation¹⁶

$$\partial^2 \Psi / \partial Z^2 + \partial^2 \Psi / \partial R^2 - (1/R)(\partial \Psi / \partial R) = 0. \quad (5)$$

For the given geometrical arrangement of the mixed system holds $H=D$ so that the dimensionless streamline function, with respect to the transformation equation (1a)–(3), is given by relations

$$W_{rad} = (1/\pi)(d/D)^2 (1/R)(\partial \Psi / \partial Z), \quad (6a)$$

and

$$W_{ax} = -(1/\pi)(d/D)^2 (1/R)(\partial \Psi / \partial R). \quad (6b)$$

* Dashed symbols represent values averaged in time.

Relation (5) may be solved in the region V_1 for the boundary condition

$$\Psi \equiv 0, \quad [R = R_0; Z \in \langle 0; Z_1 \rangle], \quad (7a)$$

$$\Psi \equiv 0, \quad [R = R_4; Z \in \langle 0; Z_3 \rangle], \quad (7b)$$

$$\Psi \equiv 0, \quad [Z = 0; R \in \langle R_0; R_4 \rangle]. \quad (8)$$

Identities (7a) to (8) are expressing mathematically validity of the assumption 4). For cross-sectional areas S_i , ($i = 1, 3$) through which liquid enters and leaves the region V_1 the boundary conditions are given by the functions

$$\Psi_i = \Psi_i(R), \quad [Z_i = \text{const.}; i = 1, 3], \quad (9)$$

which may be determined by integration of relations (6a) and (6b)

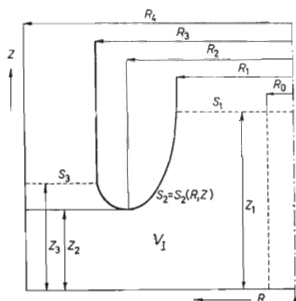


FIG. 1
Region V_1

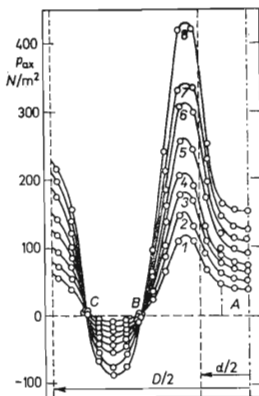


FIG. 2
Radial Profile of Axial Pressures Acting on the Vessel Bottom

Curve	1	2	3	4
Re. 10^{-4}	7.11	7.98	8.30	9.75
Curve	5	6	7	8
Re. 10^{-4}	10.65	11.52	12.50	13.40

$$\Psi_1(R) = \pi(D/d)^2 \int_{R_0}^R W_{ax,1}(R) dR, \quad (10a)$$

$$[Z_1 = \text{konst.}; R \in \langle R_0; R_1 \rangle],$$

$$\Psi_3(R) = -\pi(D/d)^2 \int_{R_4}^R W_{ax,3}(R) dR, \quad (10b)$$

$$[Z_3 = \text{konst.}; R \in \langle R_4; R_3 \rangle],$$

where for $W_{ax,i}$, ($Z_i = \text{konst.}; i = 1, 3$) are substituted values determined experimentally in areas S_1 and S_3 . With respect to validity of the continuity equation (4) for the considered region with regard to assumptions 2) and 4) equality must hold

$$\Psi(R_1, Z_1) = \Psi(R_3, Z_3) = \Psi_{\max} \quad (11)$$

and projection of plane S_2 into the plane (R, Z) is the geometrical locus of maximum values of function

$$\Psi_{\max} = \Psi_{\max}(R, Z) = \text{konst.}, [R \in \langle R_1; R_3 \rangle; Z \in \langle Z_1; Z_3 \rangle] \quad (12)$$

while the shape of the curve, which is the considered projection of the plane S_2 , must be determined. Relation (12) represents the boundary condition for the given region of arguments which together with relations (7a) to (8) and (9) gives the necessary system for solution of the partial differential equation (5). This solution, *i.e.* the first boundary problem, may be for the considered system determined by some of the standard numerical methods by a computer¹⁷. The boundary conditions for solution of the Laplace equation (5) may be determined from the radial profile of axial pressures acting on the vessel bottom. Flow of the charge creating the discussed axial pressures is flowing through the region V_1 (Fig. 1) and informations concerning this volume are obtained from the experimentally obtained¹² shape of curve $p_{ax} = p_{ax}(r)$ (Fig. 2). Other simplifying assumptions for the volume V_1 are made: 6) Liquid enters and leaves the volume V_1 through cross-sectional areas S_1 and S_3 only in the axial direction; 7) second power of velocity in each cross-sectional area S_1 and S_3 is directly proportional to the static pressure on the vessel bottom in the point of axial (vertical) projection of the considered point; 8) mass forces are negligible.

Boundaries of region V_1 are then located in the characteristic points on the diagrams of axial pressures (Fig. 2): 1) Radial coordinate R_0 (inside radius of region V_1) is given by the location of the point A on the profile of axial pressures where the derivative $\partial p_{ax}/\partial r$ changes expressively from approximately zero to non-zero value. 2) Radial coordinate R_1 (outside radius of cross-section S_1) is determined by the location

of the point B on the profile of axial pressures with the zero value of the function. 3) Radial coordinate R_3 (inside radius of cross-section S_3) is given by location of the point C on the profile of axial pressures where the value of the function is also zero. 4) Radial coordinate R_4 (outside radius of region V_1) is given by the external boundaries of axial profile of radial pressures. It has constant value $R_4 = 0.5$, since the external boundary of region V_1 is identical with the inside wall of the vessel.

With regard to assumptions (6) and (7), the cross-section area for flow at R_1 , after its reversal due to the vessel bottom, can be considered identical with the cross-sectional area S_1 , and the cross-sectional area for flow at R_3 , before its reversal due to the vessel bottom, can be considered identical with cross-sectional area S_3 . Heights Z_1 and Z_2 of cross-sections S_1 and S_3 above the bottom can be determined from the known quantities R_0 , R_1 , R_3 and R_4 by use of relations

$$Z_1 = (R_1^2 - R_0^2)/2R_1, \quad Z_3 = (0.25 - R_3^2)/2R_3, \quad (13a,b)$$

for above mentioned value of the quantity R_4 .

Radial profiles of dimensionless axial velocity component $W_{ax,i} = W_{ax,i}(R)$, [$i = 1, 3$] can be determined in cross-sections S_1 and S_3 from the corresponding profiles of axial pressures at the bottom across the considered regions. If the change of flow direction caused by the plane bottom equals to $\pi/2$, we can write with respect to assumption (7)

$$2\pi p_{ax}(r) r dr = 2\pi \rho \bar{w}_{ax}^2(r) r dr, \quad (14)$$

so that the axial velocity component at the point r equals to

$$\bar{w}_{ax}(r) = [p_{ax}(r)/\rho]^{1/2}. \quad (14a)$$

If we introduce the dimensionless pressure on the bottom by

$$P_{ax} \equiv p_{ax}/[\rho(\pi dn)^2], \quad (15)$$

Eq. (14) can be, by used of definitions (1a) and (2a), arranged into the form

$$W_{ax}(R) = [P_{ax}(R)]^{1/2}. \quad (16)$$

In this way, the basis can be obtained for solution of Eqs (10a) and (10b) from which follows the dimensionless stream function Ψ in cross-sections S_1 and S_3 . Maximum values of the flow function Ψ_{\max} are reached in the point $R = R_1$ as well as in the point $R = R_3$. The curve $\Psi_{\max} = \Psi_{\max}(R, Z)$ thus represents the projection of the wall of stream tube, i.e. part of the boundary of region V_1 . From the radial

profile of the quantity p_{ax} between points B and C (Fig. 2) follows that its characteristics is different from that in regions below cross-sections S_1 and S_3 . There the flow is considered to be already directed after the reversal of the charge at the bottom, and the profile $p_{ax} = p_{ax}(r)$ indicates the average energy relations in the flow. This region can be divided into two sub-regions limited partially by cylindrical surfaces with radii $R_1(r_1, \text{resp.})$ and $R_2(r_2, \text{resp.})$, partially by cylindrical surfaces with radii $R_2(r_2, \text{resp.})$ and $R_3(r_3, \text{resp.})$ and by the area $S_2 = S_2(R, Z)$. Location of r_2 on the radial jet is considered in that point of profile $p_{ax} = p_{ax}(r)$ in which the quantity p_{ax} has its minimum, *i.e.* where simultaneously holds

$$(\partial p_{ax} / \partial r)|_{r=r_2} = 0, \quad (17a)$$

$$(\partial^2 p_{ax} / \partial r^2)|_{r=r_2} > 0. \quad (17b)$$

These relations are with regard to definitions (1a) and (15) valid as well as for dimensionless quantities R and P_{ax} . From Fig. 2 it followed, that the mentioned point on the radial profile of axial pressures may be easily located.

For sub-regions limited by area $S_2 = S_2(r, z)$ or $S_2 = S_2(R, Z)$ we write the Bernoulli equation for real liquid and the continuity equation^{16,18}

$$\overline{\overline{gz_1}} + \overline{\overline{p_{st,1}/\rho}} + \overline{\overline{w_1^2/2}} = \overline{\overline{gz(r)}} + \overline{\overline{p_{st}(r)/\rho}} + [1 + \overline{\overline{\xi_1(r)}}] \overline{\overline{w(r)^2/2}}, \quad (18a)$$

$$2\pi r_1 z_1 \overline{\overline{w_1}} = 2\pi r z(r) \overline{\overline{w(r)}}, \quad (18b)$$

$$\overline{\overline{\xi_1(r)}} = c[1 - \overline{\overline{w_1/w(r)}}]; \quad r \in \langle r_1; r_2 \rangle, \quad (18c)$$

$$\overline{\overline{gz(r)}} + \overline{\overline{p_{st}(r)/\rho}} + \overline{\overline{w(r)^2/2}} = \overline{\overline{gz_3}} + \overline{\overline{p_{st,3}/\rho}} + [1 + \overline{\overline{\xi_3(r)}}] \overline{\overline{w_3^2/2}}, \quad (19a)$$

$$2\pi r z(r) \overline{\overline{w(r)}} = 2\pi r_3 z_3 \overline{\overline{w_3}}, \quad (19b)$$

$$\overline{\overline{\xi_3(r)}} = [(\overline{\overline{w(r)}} - \overline{\overline{w_3}})/\overline{\overline{w_3}}]^2; \quad r \in \langle r_2; r_3 \rangle. \quad (19c)$$

Dotted-lines above quantities in the given equations represent average values across the considered cross-sectional area for flow characterized by the radial coordinate r .

In the first sub-region of the oriented flow reversal along the bottom (between locations r_1 and r_2) is considered reduction of its axial coordinate z , by contraction of the cross-sectional area and in the second sub-region (between locations r_2 and r_3) is, on the contrary, considered expansion of the cross-sectional area along the bottom caused by increase of its axial coordinate z . In point $r = r_2$ is the system of equations (18) and (19) valid simultaneously – the contraction of the cross-sectional

area is the largest. If we introduce, similarly as by definitions (2a) and (2b), the dimensionless velocities

$$W_i = \overline{w_i} / \pi dn, \quad [i = 1, 3], \quad (20a)$$

$$W(r) = \overline{w(r)} / \pi dn; \quad (20b)$$

and if with regard to assumption (7) we can write

$$\overline{p_{st,1}} - \overline{p_{st}(r)} = p_{ax}(r), \quad [r \in \langle r_1; r_2 \rangle], \quad (21a)$$

$$\overline{p_{st,3}} - \overline{p_{st}(r)} = p_{ax}(r), \quad [r \in \langle r_2; r_3 \rangle], \quad (21b)$$

the systems of equations (18) and (19) can be solved for the height of flow $Z(R)$, in point R along the vessel bottom. According to assumption (8) and with regard to equations (21a) and (21b) and by use of definitions of dimensionless quantities (1a), (1b), (15) and (20a,b), the solution of systems (18) and (19) can be written in the form

$$W(R) = ((c/2) W_1 + \{(c^2/4) W_1^2 + (1+c)(W_1^2 - 2P_{ax}(R))\}^{1/2}) / (1+c), \quad (22a)$$

$$Z(R) = Z_1 R_1 W_1 / W(R) R; \quad R \in \langle R_1; R_2 \rangle, \quad (22b)$$

$$W(R) = W_3 - P_{ax}(R) / W_3, \quad (23a)$$

$$Z(R) = Z_3 R_3 W_3 / W(R) R; \quad R \in \langle R_2; R_3 \rangle. \quad (23b)$$

For contraction of the tube the constant c in Eq. (18c) equals to¹⁸ $c = 0.45$. Quantities W_1 and W_2 are the average liquid velocities in the cross-sectional area of the cylinder jacket of radius R_1 and height Z_1 , or of radius R_3 and height Z_3 . With regard to validity of assumptions (6) and (7), the mentioned velocities equal to average velocities across the cross-sectional areas S_1 or S_3 . Therefore they can be calculated from absolute values of total axial forces f_{ax1} and f_{ax3} acting in cross-sectional areas S_1 and S_2 which are calculated by integration of profiles of radial pressures across the vessel bottom corresponding to the cross-sections S_1 and S_3 . Dimensionless quantities corresponding to f_{ax1} and f_{ax3} are defined by relations

$$F_{ax1} \equiv |f_{ax1}| / [\varrho(\pi dn)^2 D^2], \quad (24a)$$

$$F_{ax3} \equiv |f_{ax3}| / [\varrho(\pi dn)^2 D^2] \quad (24b)$$

and for calculation of dimensionless average velocities W_1 and W_3 we have

$$W_1 = [F_{ax1}/\pi(R_1^2 - R_0^2)]^{1/2}, \quad (25a)$$

$$W_3 = [F_{ax3}/\pi(0.25 - R_3^2)]^{1/2}. \quad (25b)$$

Eqs (25a) and (25b) represent the force with which the charge acts on the bottom in the regions of the cross-sectional areas S_1 and S_3 when, according to the assumption (6), the change of the charge direction which is acting by a force on the bottom, takes place under angle $\pi/2$ in both cases.

EXPERIMENTAL

The axial pressures on the vessel bottom were considered as the dependent variable with radial distribution used for determination of the field of streamlines in the charge flowing above the bottom. Velocities and pressures in this area were measured directly by the oriented Pitot tubes and were used for verification of the proposed model.

The above discussed characteristics of the flowing charge were measured under different geometrical arrangement of the mixed system given by the size of the used axial mixer and by its distance from the bottom and the charge surface at rest. Dynamic viscosity and density of the charge were measured as well. In the experiments, the number of the mixer revolution was varied but it was dependent both on geometrical conditions of the mixed system and on material properties of the charge. But all these quantities could have been considered, in respect to the axial pressures on the bottom as well as to the velocity and the pressure in an arbitrarily chosen point of the system, independent variables and were fixed or determined in both types of the experiments in the same way to enable comparison of the experimental results. By this procedure also the eventual different accuracy of measurement of these quantities did not affect unfavourably in comparison of dependent variables expressed in a dimensionless form. A great attention was already paid^{4,5,7,8,12} to the description of measurement of the dependent variables. All experiments were carried out in the model equipment consisting of a cylindrical vessel made of perspex with a flat bottom of diameter $D = 290$ mm filled with the charge (distilled water or aqueous solution of glycerol). The height of the liquid surface at rest H was equal to the vessel diameter. The vessel was provided with four baffles, $0.1D$ wide, reaching the bottom. A mixer with six plane blades inclined under the angle 45° was used. The mixer was situated in the axis of the cylindrical vessel and its rotation was always directed so as to pump the liquid toward the bottom. Mixers of several relative sizes d/D were used and were situated in various relative distances h_2/D above the vessel bottom. Geometric characteristics: $H = D = 290$ mm, $b = 0.1D$, $d/D = 1/3; 1/4; 1/5$, $h_2/D = 0.418; 1/3; 1/4; 1/5$, $h = 0.2d$. Data on the charge are given in Table I.

By evaluating the results of experiments, the boundary conditions for solution of Eq. (5) could have been determined and compared with the velocity field determined directly in the charge flowing above the bottom. Also the effect was analyzed of geometrical arrangement of the mixed system and of material properties of the charge on the flow pattern in the region below the horizontal plane of the mixer symmetry. By methods described in papers^{4,5,7} of this series were obtained radial profiles of the total pressure measured by oriented Pitot tubes in several directions at a given axial distance from the bottom. From these pressure data were calculated radial profiles of the axial and radial vector components of the mean local velocity from which it was possible to determine the field of streamlines in the studied region V_1 of the mixed system. This field of streamlines was determined for the known velocity field, by the use of definitions (6a) and (6b) for boundary conditions (7a), (7b) and (8). Calculation of axial and radial

TABLE I
Charge Parameters

Distilled water				Aqueous soln. of glycerol			
$\rho = 988 \text{ kg cm}^{-3}, \eta = 0.55 \text{ cP}$				$\rho = 1084 \text{ kg m}^3, \eta = 2.5 \text{ cP}$			
d/D	1/5	1/4	1/3	d/D	1/5	1/4	1/3
Re. $\cdot 10^{-4}$	13.1	14.2	13.9	Re. $\cdot 10^{-4}$	3.16	3.42	3.37
Distilled water				Aqueous soln. of glycerol			
$\rho = 1000 \text{ kg m}^{-3}, \eta = 1.0 \text{ cP}$				$\rho = 1143 \text{ kg m}^{-3}, \eta = 8.5 \text{ cP}$			
d/D	1/5	1/4	1/3	d/D	1/5	1/4	1/3
Re. $\cdot 10^{-4}$	7.27	7.87	7.76	Re. $\cdot 10^{-4}$	0.979	1.06	1.05
	7.30 ^a	7.92 ^a	7.80 ^a				

^a Total pressures measured by oriented Pitot tubes. Other conditions for axial pressures measured on the vessel bottom.

profiles of the stream function ψ and the estimate of its accuracy resulting from the accuracy of measurements by the oriented Pitot tubes was the same as was described and discussed in the already published paper⁸ of this series.

By the procedure described in papers^{12,15} of this series were obtained radial profiles of axial pressures acting on the flat bottom of the vessel. From these profiles, measured in the given mixed system on the bottom between two adjacent radial baffles, was calculated the arithmetic mean for the given position on the radial ray (*i.e.* for the identical radial distance). This mean quantities were transformed into a dimensionless form by Eq. (15). For the given charge (characterized by its kinematic viscosity η/ρ) the values of dimensionless axial pressures were then averaged for all numbers of revolutions used. In such a way obtained radial profiles of dimensionless axial pressures on the vessel bottom were plotted graphically (*i.e.* in dependence on the dimensionless radial coordinate R) from which the values of radial coordinates of boundaries of the region V_1 were read off: coordinates R_0, R_1, R_2 and R_3 . Axial coordinates Z_1 and Z_3 of the areas S_1 and S_3 were then calculated. By use of Eqs (13a) and (13b). Absolute values of axial forces f_{ax1} and f_{ax3} acting on regions of the bottom S_1 and S_3 were calculated from the experimental radial profiles $p_{ax} = p_{ax}(r)$ by the use of relations

$$|f_{ax1}| = 2\pi \int_{R_0D}^{R_1D} p_{ax}(r) r dr, \quad (26a)$$

$$|f_{ax3}| = 2\pi \int_{R_3D}^{0.5D} p_{ax}(r) r dr, \quad (26b)$$

where in Eq. (26b) was taken into account that $R_4 = 0.5$. These absolute values were then transformed by Eqs (24a) and (24b) into F_{ax1} and F_{ax3} . From these values were then, similarly as

for profiles $P_{ax} = P_{ax}(R)$, calculated the arithmetic means for the given charge and mixed system from results of measurements made at several numbers of mixer revolution. From thus obtained dimensionless axial forces the mean dimensionless velocities W_1 and W_3 in the cross-sections S_1 and S_3 by Eqs (25a) and (25b) were calculated.

From radial profiles of the dimensionless axial pressure on the bottom $P_{ax} = P_{ax}(R)$, plotted graphically, were calculated by the use of relation (16) the radial profiles of the dimensionless axial velocity component in the cross-sections S_1 and S_3 under given conditions in the mixed system. From these profiles were calculated by numerical integration radial profiles of the dimensionless stream function Ψ in the given boundaries — see Eqs (10a) and (10b). Velocities W and heights Z were calculated of relations (2b), (22) and (23).

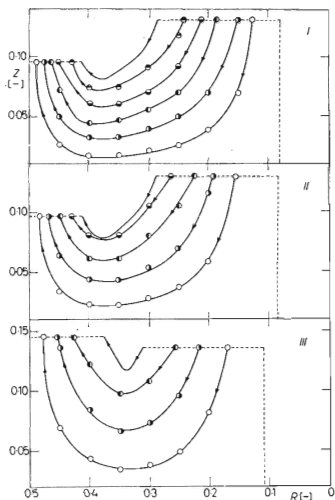


FIG. 3

Field of Streamlines in the Region V_1 ($d/D = 1/3$; $Re = 13.90 \cdot 10^4$) Calculated from Radial Profiles of Axial Pressures on Vessel Bottom

I $h_2/D = 1/4$, $\Psi_{max} = 0.143$; II $h_2/D = 1/3$, $\Psi_{max} = 0.110$; III $h_2/D = 0.418$ $\Psi_{max} = 0.095$.

Point Ψ 0-025 0-050 0-075 0-100 0-125 0-150

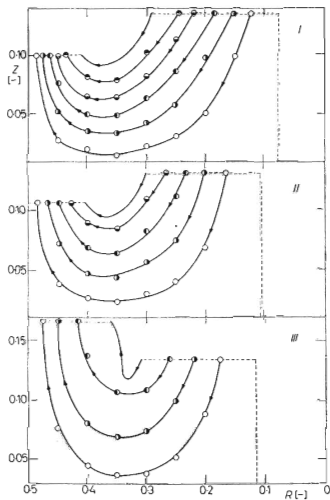


FIG. 4

Field of Streamlines in the Region V_1 ($d/D = 1/3$; $Re = 7.76 \cdot 10^4$) Calculated from Radial Profiles of Axial Pressures on Vessel Bottom

I $h_2/D = 1/4$, $\Psi_{max} = 0.149$; II $h_2/D = 1/3$, $\Psi_{max} = 0.115$; III $h_2/D = 0.418$, $\Psi_{max} = 0.094$.

Point Ψ 0-025 0-050 0-075 0-100 0-125 0-150

Boundary conditions for solution of Eq. (5) across the region V_1 are given partially by position of their boundaries, partially by the shape of the stream function between cross-sections S_1 and S_3 . Accuracy with which all these quantities are determined depends first of all on accuracy with which the radial profiles of axial pressures and the corresponding axial forces acting on the respective parts of the bottom are determined and how adequate is the proposed model. Coordinates of boundaries of region V_1 , which can be considered exactly determined, are the axial coordinates of the bottom ($Z = 0$) and the radial coordinates of the internal surface of the vessel wall ($R_4 = 0.5$). Accuracy with which other quantities affecting solution of Eq. (5) are determined is not absolute but can be estimated with respect to accuracy of the experiments made. Accuracy of determination of the boundaries of the region V_1 : Quantity R_1 , relative accuracy $\pm 1\%$; R_3 , $\pm 1\%$; Z_3 , $\pm 1\%$; R_0 , $\pm 3\%$; R_2 , $\pm 2\%$. Accuracy of determination of the velocity field on the boundaries of the region V_1 : Quantity F_{ax1} , relative accuracy $\pm 2.5\%$; F_{ax3} , $\pm 2.5\%$; W_1 , $\pm 2.0\%$; W_3 , $\pm 2\%$; p_{ax} , $\pm 5\%$ ($Re > 10^4$); p_{ax} , $\pm 10\%$ ($Re \approx 10^4$); Ψ_{max} , $\pm 5\%$ ($Re > 3 \cdot 10^4$, $h_2/D \leq 1/3$); Ψ_{max} , $\pm 10\%$ ($Re > 3 \cdot 10^4$, $h_2/D > 1/3$); Z , $\pm 5\%$ ($R \in \langle R_1; R_3 \rangle$, $\Psi = \Psi_{max}$).

All these facts resulted in radial profiles $Z = Z(R)$, ($\Psi = \Psi_{max}$) which were continuous in the regions $\langle R_1; R_2 \rangle$ and $\langle R_2; R_3 \rangle$ but in the point $R = R_2$ a step change up to $\Delta Z = 0.01$ appeared. This difference is, with respect to accuracy with which Z_1 and Z_3 are determined, quite comprehensible but nevertheless the dependence $Z = Z(R)$, ($\Psi = \Psi_{max}$) had to be graphically smoothed with regard to the mentioned discontinuity across the whole region S_2 . It can be summarised that curves $Z = Z(R)$, ($\Psi = \Psi_{max}$) characterizing projection of the area $S_2 = S_2(R, Z)$ were determined with ± 0.015 accuracy in the direction of axis Z .

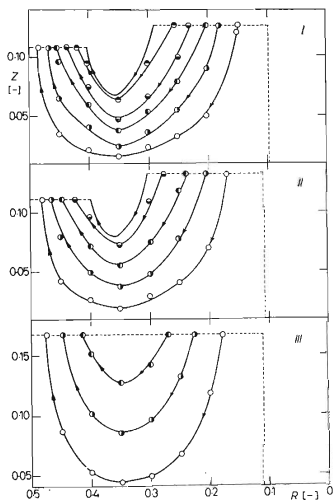


FIG. 5

Field of Streamlines in the Region V_1 ($d/D = 1/3$; $Re = 3.37 \cdot 10^4$) Calculated from Radial Profiles of Axial Pressures on Vessel Bottom

I $h_2/D = 1/4$, $\Psi_{max} = 0.137$; II $h_2/D = 1/3$, $\Psi_{max} = 0.113$; III $h_2/D = 0.418$, $\Psi_{max} = 0.100$.

Point Ψ \circ \bullet \odot \ominus $\omin�$ \bullet
 Ψ 0.025 0.050 0.075 0.100 0.125 0.150

The Laplace partial differential equation (5) was solved numerically with boundary conditions (7a), (7b)–(9) and (12) by the overrelaxation method¹⁹. The solution was modified for eventual variation of coordinates of boundaries of the considered region as values of the coordinates characterizing the boundaries of the region V_1 were changing. According to the preliminary tests, the size of increments of numerical solution was chosen $\Delta R = \Delta Z = 0.005$. For the given division and required accuracy of calculation given by the mean difference between results of two consecutive iterations $\varepsilon = 5.0 \cdot 10^{-5}$, the calculation took approximately 2.5 minutes by the computer Elliott 503 for one configuration of the region V_1 . The described numerical calculation resulted in values of the stream function in nodes of the mesh from which by interpolation the coordinates of individual streamlines could have been obtained *i.e.* curves with constant value of the stream function Ψ , corresponding to the mentioned boundary conditions.

RESULTS AND DISCUSSION

Fields of streamlines determined in the region V_1 from radial profiles of axial pressures by use of the proposed model and from the velocity field measured directly in this region can be compared. The corresponding axial profiles of the dimensionless stream function Ψ are compared for the given mixed system and material properties of the charge by use of the mean relative deviation:*

$$\Delta = \frac{100}{n+1} \sum_{k=0}^n \left| \frac{\Psi_{\text{exp},j}(Z_k) - \Psi_j(Z_k)}{\Psi_{\text{exp},j}(Z_k)} \right|, \quad [R_j \in \langle R_0; R_4 \rangle]. \quad (27)$$

From the results of this comparison the defined relative deviations fall into the range of 0–50%, while their mean values in the given axial profile are for compared cases in the range of 9–31%. Deviation of the quantity Ψ from quantity Ψ_{exp} is systematic: actual value of the stream function is larger than that resulting from the model. Mean values of quantity Δ for $d/D = 1/3$, $h_2/D = 1/4$, $\text{Re} = 7.76 \cdot 10^4$, $Z_1 = 0.136$, $Z_2 = 0.1$ are for region $Z \langle 0-0.13 \rangle$: for $R = 0.1$, $\Delta = 21.3\%$; $R = 0.15$, $\Delta = 15.5\%$; $R = 0.2$, $\Delta = 29.2\%$; $R = 0.25$, $\Delta = 30.8\%$; $R = 0.3$, $\Delta = 26.0\%$; $R = 0.35$, $\Delta = 20.0\%$; $R = 0.4$, $\Delta = 15.8\%$; $R = 0.45$, $\Delta = 8.6\%$. Mean values of quantity Δ , for the studied mixed system are: for $d/D = 1/3$, $\Delta = 20.9\%$; $d/D = 1/4$, $\Delta = 21.2\%$; $d/D = 1/5$, $\Delta = 20.9\%$.

On basis of these results the field of streamlines in the region V_1 can be constructed by use of radial profiles of axial pressures acting on the vessel bottom, with an average accuracy of 21%. This accuracy can be considered sufficient for calculations of the heat or mass transfer intensity in the region of the vessel bottom in the design of mechanically mixed process units.

Validity of Simplifying Assumptions for Flow of the Charge in the Region V_1

The mixed charge is incompressible as liquids are used (*i.e.* water or aqueous solutions of glycerol) which is characterized by the respective value of quantity $(\partial V/\partial p)_T = \text{const.}^{17}$.

* Axial coordinate Z_0 is here considered on the bottom, $Z = 0$.

Axial symmetry of the mixed system formed by a cylindrical vessel provided with radial baffles and axially situated axial mixer does not in fact exist. However, with regard to the bottom area which is affected by radial baffles it is possible to neglect this deformation of the velocity field. The effect of baffles is most profound in the region below the cross-section S_3 , while in the region below cross-section S_1 and in most cases also in the region below the cross-section S_2 there is no dependence of axial pressures on location of the radial jet between the baffles. Baffles are affecting in the part of the region V_1 below cross-section S_3 first of all location of the boundary R_3 (and partly of R_2 as well) which is dependent on location of the radial jet. Baffles are also affecting directly values of the measured axial pressures which in corresponding points of radial jets between two neighbouring baffles differ by up to 10%. By averaging these values with values in other radial jets (as we have done), mean values can be obtained and their standard deviations are according to our estimate not worse than 3%. A certain asymmetry in the region below the cross-section S_3 can be in this way eliminated by averaging the values of experimental axial pressures. Then, neither the flow rates across the mentioned regions do vary, due to the system asymmetry, by more than $\pm 3\%$. It can be concluded that the field of streamlines, with the exception of the area in close vicinity of the baffles, can be considered axially symmetric in the whole region V_1 . By this conclusion can be analogically considered the whole space of the mixed charge since neither configuration nor the flow conditions in the remaining part of the system differ from region V_1 (ref.^{5,8}).

Flow of the mixed charge was steady as the experiments were considerably longer than the time necessary for bringing the charge from the standstill into motion²⁰. At the assumption of quasi-stationary turbulent field (which is usually *e.g.*²¹ for ordinary types of turbulence fulfilled), the experiments had to be at least by three orders longer than the slowest velocity fluctuations²².

The assumption of value V_1 being a closed system is correct due to the accuracy with which the distribution of axial pressures on the vessel bottom is determined especially with respect to above mentioned asymmetry of the region below the cross-sectional area S_3 . Greater deviations at at $Re \approx 1.0 \cdot 10^4$, for $h_2/D > 1/4$, and at $Re \approx 3.0 \cdot 10^4$, for $h_2/D > 1/3$, seem to be the result of a greater effect of the charge viscosity where deceleration of the flow in the region below the area S_2 already originates gradual reversal of liquids layers, *i.e.* the charge leaves the volume V_1 already *via* area S_2 . The obtained results on velocity distribution boundaries of the region V_1 (namely, across the cross-section S_3) were therefore corrected by averaging values of quantity Ψ_{\max} at the points R_1 and R_3 . Deviation from reality, especially in the region of this cross-section, is higher than in those cases where such correction was unnecessary. From this also results limitation of the used measuring method if because of viscosity charge assumption 4) cannot be considered as adequate. It is necessary to point out that results, in which the boundary R_2 is not found, also cannot be evaluated by the proposed procedure since the force acting in the region S_1 overlaps the force acting in the region S_3 and it is therefore impossible to determine reliably boundaries of the considered volumes. This limiting condition has already been mentioned in the analysis of force action of the charge on the bottom¹⁵ and should also be taken into consideration.

Basic condition for use of the Laplace equation (5) for description of flow in the considered system is the existence of irrotational flow in the region V_1 . It is obvious that this assumption cannot be fulfilled in the charge below the plane of symmetry of the axial mixer. Failure to meet this assumption is the main reason for deviation between the theoretically determined and experimentally found streamlines fields, especially with regard to differing profiles $\Psi_j = \Psi_j(Z)$, ($R_j = \text{const.}$), which for the case of solution of Eq. (5) are linear, while in fact they are not straight as the velocity profile is pushing the streamlines closer together in direct vicinity of the bottom.

For location of the cross-sections S_1 and S_2 assumption 6) can be considered fulfilled. This follows from results of measurements of the velocity field in the charge between the mixer and

vessel bottom. A certain systematic deviation appears close to the outside boundary of the region S_1 (radius R_1), where a gradual reversal of layers of the liquid stream from downward to horizontal direction due to the vessel bottom already takes place. With respect to numerical solution of Eq. (5) and to information obtained from radial profiles of axial pressures, it was impossible to remove this shortcoming in the solution itself.

Assumption 7) results from modelling of the pressure effects accompanying a change in direction of a very thin free jet (streamline) in a considered point under vertical impact on the vessel bottom. Of course, this grossly simplifies the studied system and the results of measurements of velocity and pressure fields between the rotating mixer and the vessel bottom⁴⁻⁷ have demonstrated, that this assumption is not quite fulfilled. In the mentioned region the value of directly measured static pressure differs considerably from the hydrostatic pressure. This means that especially the cross-sectional area S_1 need not equal to the cross-sectional area for flow in the point R_1 after reversal of the stream due to the bottom and thus the quantity Z_1 calculated from relation (13a) is not correct. This concerns as well the coordinate Z_3 , the cross-section S_3 and consequently the coordinates of curve $Z = Z(R)$, ($\Psi = \Psi_{\max}$), i.e. projection of the area S_2 . The profiles $W_{ax,1} = W_{ax,1}(R)$, ($d/D = \text{const.}$, $Z_1 = \text{const.}$), as well as the coordinate R_1 calculated on basis of the discussed assumption, are proving the above given results as they do not correspond to the respective radial profiles determined from direct velocity and pressure field measurements. This is in spite of the fact that from the flow rates of the charge above the bottom determined by use of the experimental radial profiles of axial pressures above the bottom, a sufficient agreement has been obtained with the flow rate resulting from direct measurements of the velocity and pressure fields by the oriented Pitot tubes¹⁵. Point Z_1 is therefore located (determined only from values of coordinates R_0 and R_1) considerably lower than results from relation (13a) and the same can be said about location of the point Z_3 (determined from values of the coordinates R_3). In the latter case, however, the deviation from actual value is not great since axial profiles of quantities Ψ and Ψ_{exp} in the region below area S_3 are in a good agreement. On the contrary axial profiles of the discussed quantities have the greatest deviations in the points where the radial coordinate is close to the coordinate R_1 : values Ψ_{exp} are up to 50% greater than the corresponding values of Ψ .

The above discussed disagreement plays perhaps the greatest role in deviations of the fields of streamlines in region V_1 based on the proposed model and those determined experimentally. Since it is impossible to determine from axial profiles of radial pressures the non-zero value of Δp_{st} without additional measurements in the flowing charge, the last assumption must have been introduced. This is because we intended to have the complete solution based only on a single information: radial profile of axial pressures acting on the bottom. In spite of the mentioned shortcoming, further experimental studies (usually very time-consuming) are not necessary; of course the results are affected by the above given error.

Validity of assumption 8) can be verified by the field of streamlines below area S_2 , where a gradual contraction and expansion of the studied flow takes place. Streamlines, which due to the mentioned spacial changes considerably change their location, are never representing more than one third of the over-all flow rate. Changes in location of the centre of gravity of cross-sectional area are therefore not exceeding one sixth of the change of the axial coordinates Z_1 and Z_2 , or Z_2 and Z_3 which in comparison to values of the mean kinetic and potential energies of the considered flow is negligible. But it is necessary to mention here, that in case the discussed axial displacement of the centre of gravity of the flow below area S_2 must be taken into account in the solution, the direct calculation (i.e. solution of the system of Eqs (22) and (23) would change into calculation by successive approximations. Contraction of the cross-sectional area in dependence on the radial coordinate may also be used for establishing how negligible is the change

of axial position of the centre of gravity of the cross-sectional area in the stream flowing along the bottom. From the presented model the minimum height Z_2 of this stream should be in the point R_2 . This condition is in many cases not fulfilled, *i.e.* even if the radial coordinate is greater than R_2 , contraction of the cross-section area takes place. This change of contraction, though observable never exceeds the accuracy with which the dependence $Z = Z(R)$, ($\Psi = \Psi_{\max}$), is determined which is another reason for accepting the assumption 8).

Finally it can be concluded on evaluation of validity of simplifying assumptions, which are indispensable for determination of the field of streamlines from the experimental axial pressure acting on the vessel bottom, that all assumptions whose validity has been satisfactorily proved can be analogically considered to be valid practically in the whole range of the studied conditions, *i.e.* for studied geometrical arrangements of the mixed system and material properties of the charge. Further, introduction of those assumptions whose validity has not been fully proved is not motivated by insufficient understanding of mechanism of the studied operation but by an endeavour to describe the studied process by as simple relations as possible that can be solved in an adequate manner on a computer by methods of numerical mathematics *i.e.* with the required accuracy and length of calculation. The presented solution meets these requirements.

Effect of Material Properties of the Charge and Geometrical Arrangements of the Mixed System on the Flow Pattern at the Vessel Bottom

Effect of kinematic viscosity of the mixed liquid on the flow pattern at the bottom can be explained by greater dissipation of mechanical energy transformed into heat in the charge with increasing viscosity. Correspondingly, also the mean flow velocity decreases for about constant volumetric flow so that the cross-sectional area is larger than in case of the charge with a lower viscosity (Figs 3—5). At a lower mean velocity and at lower values of the velocity gradient across the considered region the rate of dissipation of mechanical energy on the one hand increases due to the increased liquid viscosity, while on the other hand it decreases due to the decreased specific kinetic energy of liquid. So the flow pattern in a mixed system is significantly affected by material properties of the homogeneous mixed liquid while the global quantities characterizing the mixed system, as *e.g.* its power input or specific power input, do not practically change¹¹. In the space below the plane of symmetry of a rotating axial mixer at turbulent flow of the charge is dissipated in average 60% of power input of the mixer⁵, though the mentioned volume represents only 1/4—1/3 of the whole charge volume. This spacial distribution of dissipation will therefore decisively affect the overall balance of mechanical energy in the whole system. From the requirement, that such conditions should be established in the system at which minimum of the energy is dissipated, results the change of shape and size of the region V_1 with increasing kinematic viscosity of the charge. This also means that some considerations concerning the ideality of liquid flowing along the bottom made earlier¹⁵, must have been corrected. It is necessary to mention here, that expansion of the region of coaxial cylinder with radius R_0 with increasing viscosity is probably related with friction forces acting in this region which are setting into the irregular motion (upward and horizontal) of the other liquid layers flowing downwards. This explanation is not contradictory to that one made earlier, concerning the growth of the region V_1 with increasing kinematic viscosity of the charge as contribution of this region to the energy dissipated by viscous friction into heat is negligible in the region below the plane of mixer symmetry. Both the energy dissipated and the mean velocity of flow are very small fractions of the corresponding quantities in the whole volume V_1 .

The relative mixer size d/D is represented by different densities of streamlines in the volume V_1 and by the shape of the considered region. The density of streamlines and thus the flow intensity

at the bottom as well increase with decreasing ratio d/D . From more than twenty five measurements, the density of streamlines is proportional to the first power of reciprocal value of this ratio. For the total volumetric flow rate at the bottom to exceed the pumping capacity of the mixer is decisive not only the mixer size but also its distance from the bottom. Shape of the region V_1 is dependent on the ratio d/D with changing diameter of the jet from the rotor region. Areas S_1 and S_3 are increasing with the increasing value of d/D (quantity R_1 is proportional to the sixth root of the ratio d/D) and the region S_2 is decreasing in the corresponding manner. The height of the region V_1 decreases as well if the ratio d/D decreases. Thus the smaller is the relative size of the mixer, the smaller are dimensions of the region V_1 while the region below the plane S_2 (where flow at the bottom prevails) is expanding. The region of cylinder of radius R_0 also decreases with the decreasing value of ratio d/D . Smaller mixer thus guarantees greater flow intensity in vicinity of the bottom with a simultaneous decrease of the "dead region" (cylinder of the radius R_0) while a larger mixer promotes flow in a greater volume of the charge but the flow intensity is smaller.

The effect of the relative distance of the mixer from the vessel bottom h_2/D is for all the studied mixer sizes the same (Figs 3–5) *i.e.* with increasing distance h_2/D the flow intensity of the charge considerably decreases in the region V_1 . From the results of experiments, it is proportional to $(D/h_2)^{0.40}$. The size of the region V_1 is frequently not affected by the change of quantity h_2/D so that the made conclusion results directly from evaluation of the experiments. But if $h_2/D > 1/3$, the size of region V_1 changes with the changing ratio h_2/D (see *e.g.* Fig. 3). Similarly with mixers of greater sizes the areas S_1 and S_3 are increasing, values of coordinates Z_1 and Z_3 are increasing as well with the region below the plane S_2 successively diminishing, *e.g.* case III in Fig. 5. The flow of the charge becomes greater with increasing of the ratio h_2/D when finally boundaries of regions S_1 and S_3 merge. Thus if $R_1 = R_2 = R_3$, a continuous reversal of liquid layers from the downward to upward direction takes place without contraction of the stream at the vessel bottom. This is also another of limiting conditions when, at a greater value of the ratio h_2/D , the proposed method for determination of the field of streamlines at the vessel bottom cannot be used any more as determination of boundaries of both streams becomes indeterminable (see also considerations made earlier). This is because reliable determination of streamlines which are and are not reaching the region of the bottom is not possible. Radius of the region in vicinity of the vessel axis where the flow is not oriented (cylinder of the diameter R_0) is increasing with increasing distance of the mixer from the vessel bottom as streamlines from the region V_1 are consecutively transferred into the considered region with a simultaneous change of their direction (*e.g.*⁴). Size of this "dead volume" (*i.e.* volume with a very slow flow of the charge) thus increases with increasing size of the region V_1 (as in the case of greater values of the ratio d/D) and the mean flow velocity there decreases.

Effect of Flow Intensity at the Bottom on Mass and Heat Transfer in the Mixed Charge

Liquid motion initiated by a rotating mixer is the usual condition for an effective handling of a mechanically mixed operation. Motion of the mixed charge itself is usually not the purpose of the operation but it includes heat and/or mass transfer as well. In the following part effect of the shape of the field of streamlines at the bottom of a mixed vessel on heat transfer between the bottom and the charge and on homogenisation rate in the charge is discussed.

Heat transfer between the bottom and the flowing charge mixed by an axial mixer was studied by Kupčík^{2,3}. According to this study the heat transfer intensity between the vessel bottom and the charge is decreasing with increasing relative distance h_2/D of the mixer from the bottom. Heat transfer coefficient between the charge and the bottom is at given hydrodynamic conditions proportional to $(D/h_2)^{0.45}$. This value is in agreement with the results obtained in this study

on the effect of h_2/D on flow intensity at the bottom. This agreement confirms that heat transfer between the charge and the bottom may be expressed by equations of forced convection, *i.e.* heat transfer mechanism which is above all affected by the intensity of liquid flow in the considered region. Similarly, the dissipative character of the flowing charge assumed by the author²³ which was later verified²⁴ can be, on basis of the analysis of radial profiles of axial pressures acting on the bottom, considered as experimentally confirmed.

Suspension of solid particles in the mixed charge represents the two-phase flow but the velocity field in the continuous phase (liquid) is decisive for the force equilibrium at which it is formed. This state given by the critical number of revolutions was studied for axial types of mixers *e.g.* by Zwietering²⁵ according to which the given quantity is proportional to $(D/d)^{1.82}$. This value is in fair agreement with the results characterizing the effect of quantity d/D on flow intensity of the charge at the vessel bottom. On their basis the conclusion can be made that a smaller mixer initiating larger flow rate at the bottom is in turbulent regime at suspension of solid particles more advantageous than a relatively larger mixer. With increase of the quantity h_2/D a decrease of the critical number of mixer revolutions can be expected. This is because with increasing distance between the mixer and bottom the flow intensity of the charge at the bottom decreases and also the radius R_0 of the "dead region" along the system axis increases. Value of the critical number of revolutions will thus obviously increase with increasing distance between the mixer and bottom.

Spacial distribution of mass transfer rates in the charge at homogenisation of miscible liquids by rotating mixers has already been studied²⁶. It has been determined that in the region below the plane of symmetry of a rotating mixer the homogenisation rate is considerably greater than above this plane. This is in agreement with the conclusions made in this study as the dissipative flow region reaches a high turbulent viscosity which is the useful condition for turbulent mass transfer. This conclusion is also in agreement with considerations made in studies on the spacial dissipation of mechanical energy in the charge with an axial mixer and radial baffles⁵ as well as studies on the dissolving rates of solid phase at mechanical mixing²⁷. Spacial homogeneity of the mass transfer rate will thus be reached with mixers situated farther from the bottom as the volume of the region in which the considered process takes place will increase at the expense of the volume where the homogenisation or dissolving rates are lower.

The authors thank Prof. H. Steidl and Dr V. Kudrna, Chemical Engineering Department, Institute of Chemical Technology, Prague I, for many interesting and valuable comments.

LIST OF SYMBOLS

- b width of radial baffle
- c constant
- D vessel diameter (m)
- d mixer diameter (m)
- f force (N)
- g gravitational acceleration (m s^{-2})
- H height of charge surface at rest above the bottom (m)
- h width of mixer blade (m)
- h_2 vertical distance of the horizontal plane of mixer symmetry from bottom (m)
- n number of elements in the system
- n number of revolutions of the mixer (s^{-1})
- p pressure (N m^{-2})
- r radial coordinate, radius (m)
- S dimensionless area

T	absolute temperature (deg)
V	volume (m^3)
V_1	volume of region where the Laplace equation is solved (m^3)
w	local liquid velocity ($m\ s^{-1}$)
z	axial (vertical) coordinate (m)
φ	angular coordinate (deg)
ϵ	maximum acceptable error of numerical solution of the Laplace Eq.
ξ	local friction factor
η	dynamic viscosity of the charge ($kg\ m^{-1}\ s^{-1}$)
ρ	density charge ($kg\ m^{-3}$)
ψ	stream function ($m^3\ s^{-1}$)
$F \equiv f /[\rho(\pi dn)^2 D^2]$	dimensionless force
$P_{ax} \equiv p_{ax}/[\rho(\pi dn)^2]$	dimensionless axial pressure
$R \equiv r/D$	dimensionless radial coordinate
$Re \equiv nd^2 \rho/\eta$	Reynolds number
$W \equiv w /\pi dn$	dimensionless velocity
$Z \equiv z/D$	dimensionless axial (vertical) coordinate
$\Psi \equiv \psi/nd^3$	dimensionless stream function

Superscripts

1	related to area S_1 of the first stream reversal at bottom
3	related to area S_3 of second stream reversal at bottom
ax	axial component
rad	radial component
max	maximum value

REFERENCES

- Rushton J. H., Oldshue J. Y.: *Chem. Eng. Progr.* **49**, 161, 167 (1953).
- Porcelli J. V., Marr G. R.: *Ind. Eng. Chem., Fund.* **1**, 172 (1962).
- Fořt I.: *This Journal* **32**, 3663 (1967).
- Fořt I., Podivinská J., Baloun R.: *This Journal* **34**, 959 (1969).
- Fořt I., Neugebauer R., Pastyříková H.: *This Journal* **36**, 1769 (1971).
- Fořt I.: *This Journal* **36**, 2914 (1971).
- Kudrna V., Fořt I., Eslamy M., Cvilink J., Drbohlav J.: *This Journal* **37**, 241 (1972).
- Fořt I., Gračková Z., Koza V.: *This Journal* **37**, 2371 (1972).
- Fořt I., Sedláková V.: *This Journal* **33**, 836 (1968).
- Fořt I., Valešová H., Kudrna V.: *This Journal* **36**, 164 (1971).
- Uhl V. W., Gray J. B.: *Mixing Theory and Practice*, Vol. I. Academic Press, New York 1966.
- Fořt I., Tomeš L.: *This Journal* **32**, 3520 (1967).
- Hixson A. W., Baum G. J.: *Ind. Eng. Chem.* **34**, 194 (1942).
- Žaloudík P.: *Thesis*. Research Institute of Macromolecular Chemistry, Brno 1964.
- Fořt I., Eslamy M., Košina M.: *This Journal* **34**, 3673 (1969).
- Kočin N. E., Kibel' I. A., Roze N. V.: *Theoretical Hydromechanics* (in Russian). Gos. Izd. Fiz. Mat. Lit., Moscow 1963.
- Robertson J. M.: *Hydrodynamics in Theory and Application*. Prentice-Hall, London 1965.

18. Bird R. B., Stewart W. F., Lightfoot E. N.: *Transport Phenomena*. Wiley, New York 1960.
19. Forsythe C. E., Wasow W. R.: *Finite-Difference Methods for Partial Differential Equations*. Wiley, New York 1960.
20. Takeda K., Hoshino T.: Chem. Eng. (Japan) 29, 506 (1965).
21. Hince J. O.: *Turbulence* (in Russian). Gos. Izd. Fiz.-Mat. Lit., Moscow 1963.
22. Sato Yu., Horie Yu., Kamiwano M., Yamamoto K.: Chem. Eng. (Japan) 31, 275 (1967).
23. Kupčik F.: *Thesis*. Research Institute of Macromolecular Chemistry, Brno 1969.
24. Fořt I., Hrubý M., Mořna P.: This Journal 38, 1737 (1973).
25. Zwietering T. N.: Chem. Eng. Sci. 8, 244 (1958).
26. Landau J., Procházka J., Václavek V., Fořt I.: This Journal 28, 279 (1963).
27. Kolář V.: *Thesis*. Institute of Chemical Technology, Prague 1958.

Translated by M. Rylek.